

HINS_SS1_SOL_02d
 Fabrication Summary and Test Results

G. Chlachidze, G. Davis, C. Hess, F. Lewis, D. Orris, R. Rabehl, M. Tartaglia,
 I. Terechkine, J. Tompkins, G. Velev, T. Wokas

I. Fabrication Summary

HINS_SS1_SOL_02d is a “Type-2” (with correctors) prototype solenoid, for the first superconducting section (hence the designation SS1) of the HINS linac. The design basis and evolution of the design (which is qualitatively similar to the CH section solenoids) is described in detail in a design note [1]. The solenoid was built from Main Coil (MC) serial number SS1_M02, and Bucking Coils (BC) SS1_B03 and SS1_B04.

In April 2008, the first SS1 section Type-1 solenoid was built and tested [2]. The Type-2 solenoid was designed by introducing corrector dipoles inside the main coil and by re-optimizing the solenoid geometry: to meet the very low SS1 section fringe field requirement, the width, height, radial and axial positions of the bucking coils needed to be optimized. Because the fringe field in the new design was as low as in the tested Type-1 device, it was decided to use this design as a universal approach to the SS1 Type-1 and Type-2 solenoids – thus making all of the solenoid coils and geometry identical whether or not dipole coils are included. Fig. 1 shows the design proposed in [1] for a Type-2 prototype solenoid.

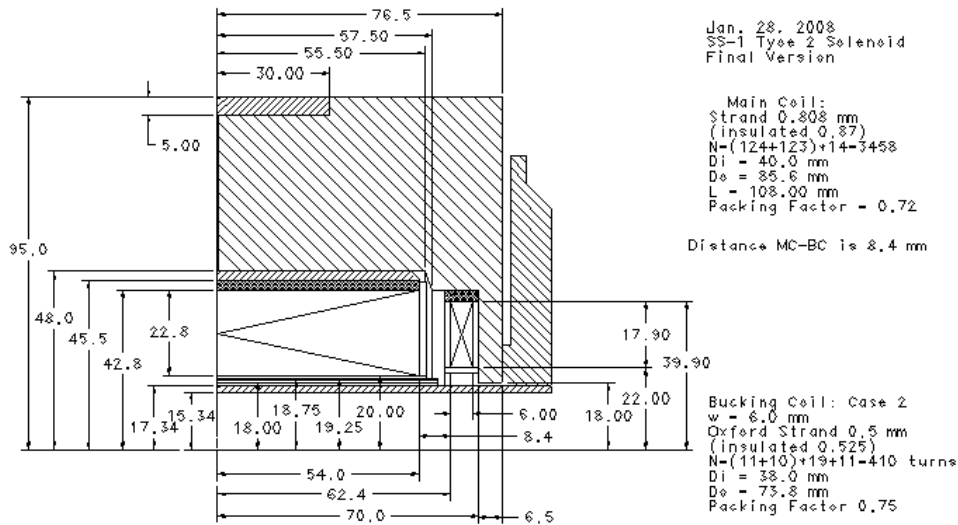


Fig. 1. SS1 Type-2 prototype solenoid proposed design.

The as-built solenoid, shown in Fig. 2, differs slightly from this, and its features will be discussed in detail.

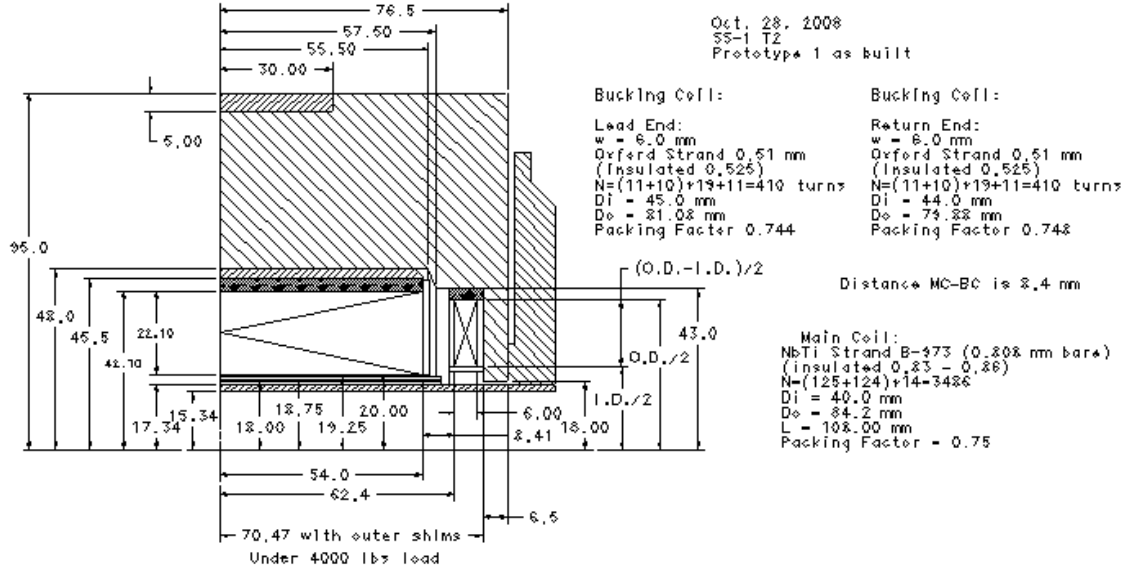


Fig. 2. As-built SS1 Type-2 prototype solenoid design.

Although the design is close to that of the Type-1 prototype in [2], some differences for the Type-2 prototype must be mentioned:

First, it was planned to wind the MC from the same strand used to build the Type-1 prototype, the SSC-type B-2199 NbTi strand with the measured critical surface given in Table 1 below. The lack of sufficient strand to make all the needed SS1-section solenoids forced us to change the strand. Instead, IGC strand reel B-973, with the measured critical surface given in Table 2, was used (and will be used for SS1 solenoid production). This strand has a significantly lower critical surface and was not chosen for use in the solenoid program before the SSC strand prepared for the fabrication was stolen near the end of 2007. Moreover, after coating at MSW, the insulated strand cross-section became slightly elliptical (insulated strand diameter was between 0.843 mm and 0.858 mm) which imposed some difficulties to the winding process (although they could be overcome). As a result the quench performance of the solenoid became somewhat degraded, ~ 5% lower. This can be seen in Fig. 3 where critical surfaces of these two strands, with the as-built solenoid load line, are compared.

Table 1: 0.808 mm strand (SSC B-2199) critical current at 4.2 K

B(T)	2	3	4	5	6	7	8	9
I (A)	1176	942	772	629	494	365	235	113

Table 2: 0.808 mm strand (IGC B-973) critical current at 4.2 K

B(T)	2	3	4	5	6	7	8	9
I (A)	848	664	540	442	356	273	191	113

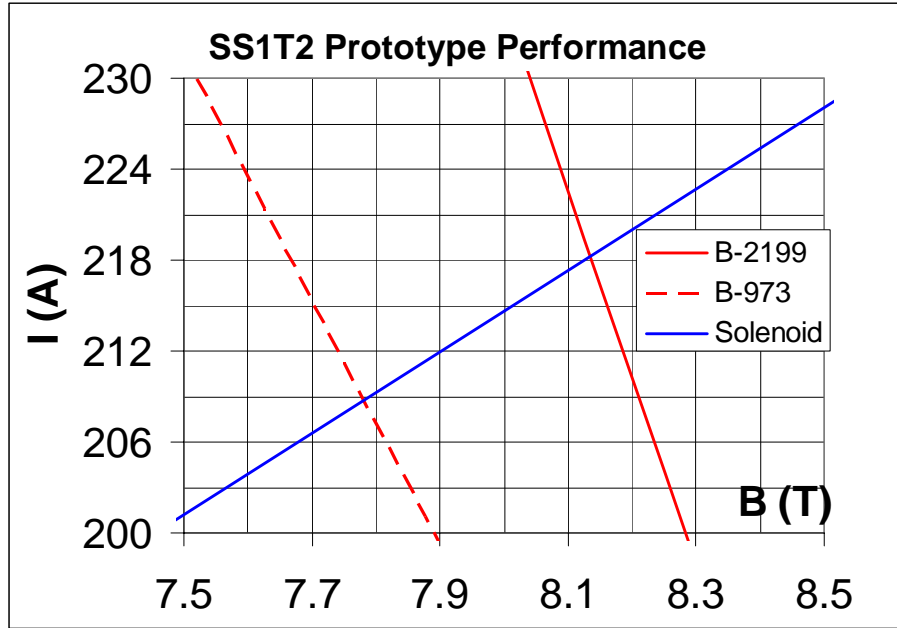


Fig. 3. Expected quench current of the SS1 prototype solenoid with different strands in the main coil at 4.2 K.

Second, because of the different strand used, the geometrical parameters of the main coils changed; the as-built parameters are shown in Table 3 below, as well as in Fig. 2.

Table 3. As-built Main Coil Parameters

Coil I.D.	40 mm
Coil O.D.	84.2 mm (average)
Coil Length	108 mm
Number of turns in the odd layers	125
Number of turns in the even layers	124
Number of layers	28
Total number of turns in the main coil	3486

Third, for this prototype we decided to vary the axial and radial positioning of the bucking coils to check the impact of these parameters on the fringe field. The distance between the bucking coil and the main coil was made 8.4 mm (8.41 measured), versus 9.0 mm in the SS1 Type-1 solenoid. The gap between the two halves of the flux return is 0.35 mm under the load of 4000 lbs.

The bucking coils were wound using the strand that was used for the SS1 Type-1 prototype [2]: Oxford 0.5 mm strand (0.525 mm insulated diameter). The strand critical surface measurements are reproduced in Table 4, and winding data for bucking coils are shown in Table 5, as well as in Fig. 2.

Table 4: 0.5 mm strand 8277-2A2B critical current at 4.2 K

B (T)	1	2	3	4	5	6	7
Im/Ic (A)	646/618	456/453	375/367	310/307	258/254	206/201	154/149

Table 5. As-built Bucking Coil Parameters

	Lead End, BCL	Return End, BCR
Coil I.D. (mm)	45	44
Coil O.D. (mm)	81.08	79.9
Coil Length (mm)	6.0	6.0
Number of turns in the odd layers	11	11
Number of turns in the even layers	12	12
Number of layers	39	39
Total number of turns in the main coil	410	410

The design and expected performance of the dipole corrector windings is described in sections IV and V of [1]. Unlike the CH section, there is no individual cryostat and warm bore tube for the SS1 section lenses: the dipole windings are therefore closer to the beam, hence more attention must be paid to make the steering field uniform. By employing a one-layer dipole-type winding on a cylindrical surface, with turns in the central part of the winding tightly laid within a $0^\circ - 60^\circ$ angle range, the steering field can be made uniform to $\sim 1\%$ inside a 10 mm radius and not exceeding 10% variation within the full aperture of 15 mm radius.

The dipole corrector coils were wound using 0.3 mm (0.33 mm insulated) strand 54S43 (Cu/nonCU = 1.3, Dfil = 25 μm) made by Supercon, Inc. Critical current of the strand is shown in Table 6. Fig. 4, taken from the design note [1], shows in detail the radial arrangement of the dipole windings (coil angles not optimized in this view), after a practice coil was made to determine the actual radial thickness required for each layer. The general layout of the horizontal corrector, is shown in Fig. 5. The optimal winding angle of 60° ensures the best magnetic field flatness within the aperture of the dipole. The length of the dipole corresponds to the length of the main coil.

Table 6: Dipole Corrector strand 54S43 performance at 4.2 K

B (T)	3	5	7	9
I (A)	100	80	45	16

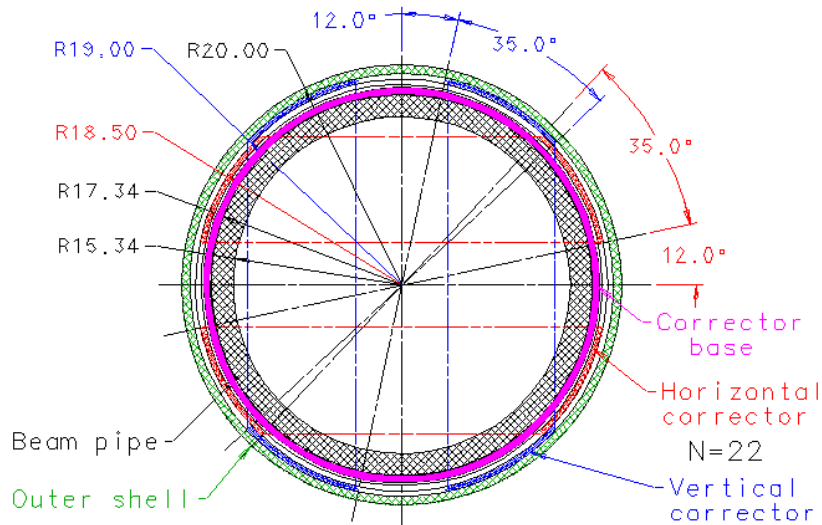


Fig. 4. Cross-section of a corrector assembly showing radial dimensions

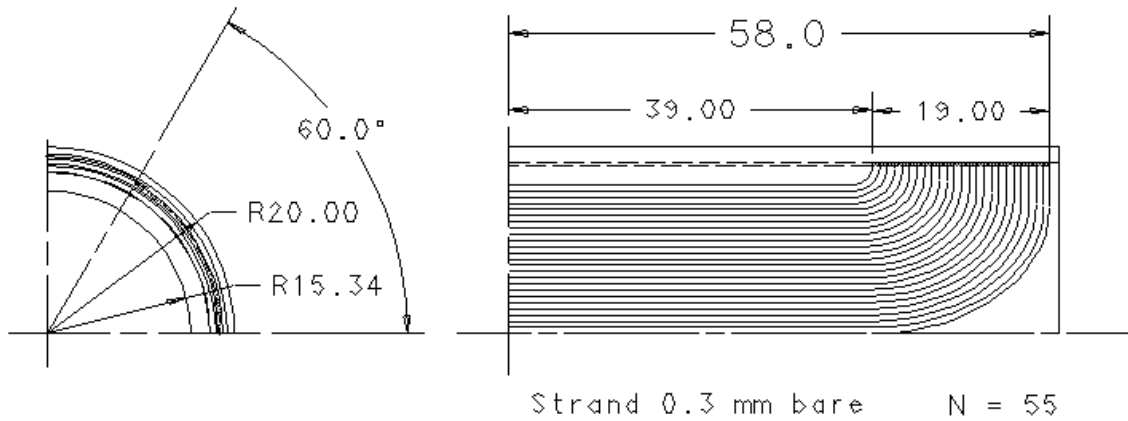


Fig. 5. General layout of the horizontal corrector.

The base for the winding is the thin-wall stainless steel tube placed above the beam pipe. The outer diameter of the base pipe is 35.9 mm. The outer diameter of the corrector assembly (40 mm) forms a base for the main coil winding. For each dipole coil, the strand was wound flat in a fixture and bonded to a substrate of thin tape, as shown in Fig. 6. The coils were then wrapped around and bonded to the Kapton-insulated base pipe; Fig. 7 illustrates the assembled prototype dipole corrector package, and Fig. 8 shows the as-built angular positions of each winding in the horizontal and the vertical dipole corrector. A 60° winding angle was the goal for the prototype solenoid, but it was difficult to keep the angular dimensions to better than a few degrees. To ensure decent field uniformity requires more than maintaining the angular dimensions of the dipole windings. The planned number of turns in each winding was 57, but practically it was difficult to make, so we ended up with 55 turns in each half-coil. The longitudinal profile of the winding differs slightly from the base design (Fig. 5): the length of the straight part of the winding is ~ 70 mm, and the total length is ~ 114 mm. Having in mind inevitable deviations from the base design parameters, performance of each steering dipole must be measured, including integrated bending strength and field uniformity.



Fig. 6. Photo of one vertical dipole half-coil after winding.



Fig. 7. Assembled SS1 prototype corrector dipole package (without outer G10 sleeve).

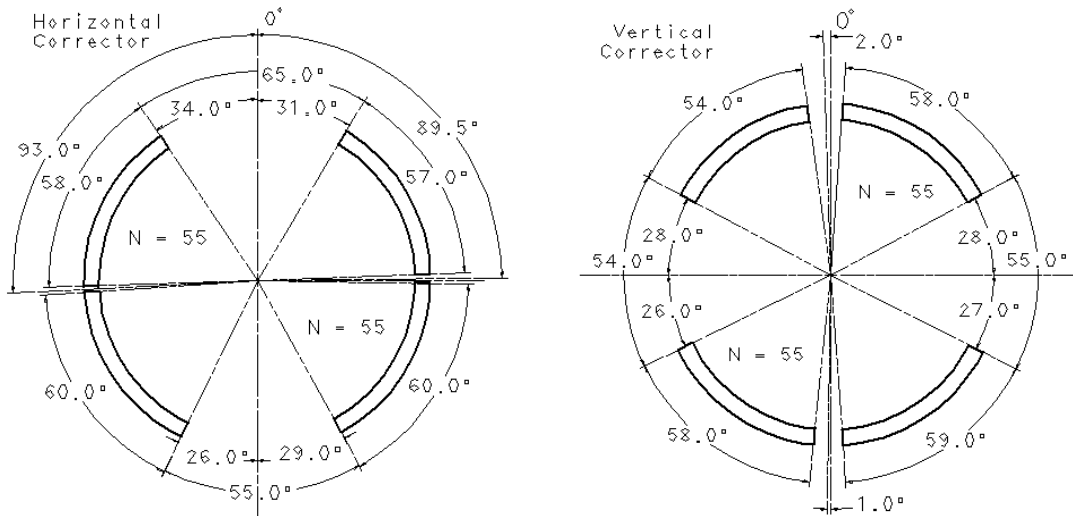


Fig. 8. As-built angular positions of the windings in the horizontal and vertical corrector.

II. Expected Quench Performance

Due to recent test stand modifications (see section III), the helium temperature during quench testing was slightly higher than the 4.2 K at which strand critical current parameters ($10^{-14} \Omega\text{-m}$ criterion) were measured. The calculated strand quench currents are predicted for the actual Test Stand 3 helium temperature (4.432 K) using the Bottura NbTi critical surface parameterization [3]. The load lines are based upon an Opera 2D model with as-built dimensions (at 300 K), with a yoke modeled by Opera-default non-linear soft iron BH material properties, and assumed to have a 0.2 mm gap at cold (0.35mm at 300 K) at the center line. Thus, as shown in Fig. 9, the limiting quench at 4.43 K is expected to occur in the Main Coil at a current of 201 A.

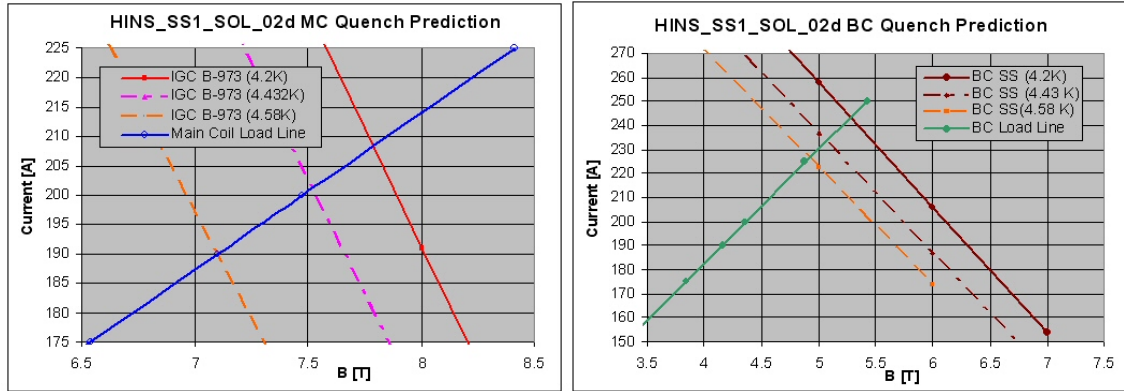


Fig. 9. Quench diagram showing peak field load lines and short sample critical surfaces for Main Coil (MC) and Bucking Coils (BC) in the as-built solenoid.

The steering correction dipole (CD) quench performance is a function of the main solenoid magnetic field in which it operates (taken to be at the radii shown in Fig. 4). Fig. 10 shows the predicted performance with the solenoid operating at 190 A. The graph predicts the dipoles quench at 44 A in 4.2 K conditions, and 39 A at the stand 3 operating temperature of 4.432 K. The stand 3 power system current read-back (calibrated to 0.1%) indicates the actual solenoid current to be 188 A when 190 is requested. Thus, the true expected quench current under test operating conditions is 40 A.

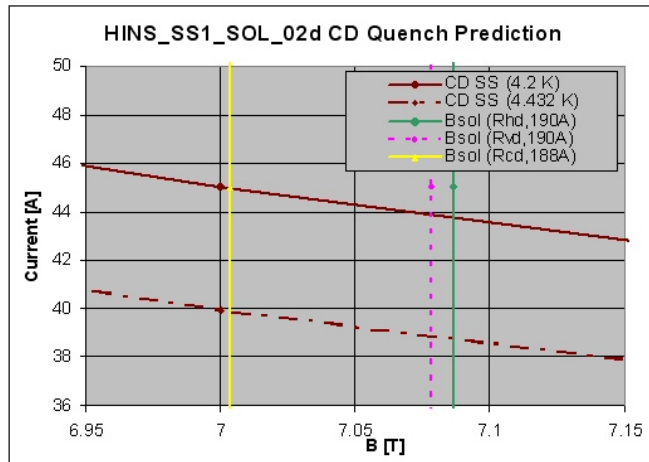


Fig. 10. Correction Dipole (CD) short sample curve and quench currents for solenoid powered at 188 and 190 A, for 4.2 K and 4.432 K test temperatures.

III. Quench Protection Issues

Earlier (in 2007) the SS1 solenoid quench protection issues were investigated in [4], [5]. In the beginning of 2008, in order to save on the required amount of superconducting strand, the design of the solenoid was modified to make it shorter - thereby reducing the quench current margin. This made the magnet geometry closer to that of the CH-type solenoids; the quench protection (QP) problem became simpler to solve.

In this section, the main result of remodeling the QP for the system are presented. The same QP analysis program [5] was used with the new winding data for the main and the bucking coils. Only quench in the bucking coil was investigated because it presents potentially the most dangerous situation. Based on the previously [4] obtained results,

only 200 A current case was investigated with the quench initiating point in the middle of the inner side of the bucking coil; in this case the maximum temperature and the voltage to ground were generated in the bucking coil. Fig. 11 below shows a summary graph of the maximum voltage in the main coil and the bucking coil versus the value of the dump resistor [6].

The optimal value of the resistor is ~ 1.5 Ohm. In this case the voltage in any part of the system never exceeds 300 V, which is considered acceptable. The maximum temperature in the bucking coil reaches ~ 210 K if a dump is not used and it is ~ 145 K with the optimal dump. Also, with the optimal dump, $\sim 50\%$ of the energy stored in the solenoid (5.5 kJ at 200 A) is dissipated in the dump resistor thus reducing LHe consumption.

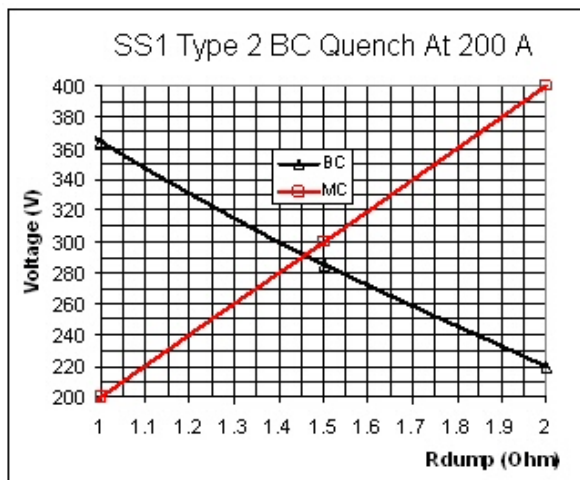


Fig. 11. Calculated maximum voltage to ground versus the value of the dump resistor for the worst-case quench scenario.

III. Test Overview

Some major changes to improve Test Stand 3 and the quench protection/power systems were made and were commissioned into operation starting in early September 2008 (with re-testing of the first three production CH solenoids): 1) a new helium transfer line with supply control valve was installed from the distribution box to stand 3, and plumbing to return helium vapor to the refrigerator compressors (along with an oxygen contamination monitor); these modifications made it possible to fill and operate the dewar using the MTF refrigerator (rather than 500-liter dewars), and provide much more flexibility in scheduling, and efficiency in operating the cold tests. 2) the quench protection and power systems were upgraded with a better current control program capable of driving multiple power supplies (useful for dipole corrector powering simultaneously with the solenoid).

The cool down of HINS_SS1_SOL_02d started on 11/11/08, and cold testing began 11/12 and continued through 11/14. Temperature of He was very stable at 4.432 K during quench testing – somewhat warmer than the 4.2 K in previous R&D tests because the new cryogenic configuration introduces a slight positive pressure in the dewar (it is limited on the low end by the refrigerator suction pressure). Because the SS1 solenoid bore is smaller than that of the CH solenoid, no warm bore was installed. Instead, for magnetic measurements, a G-10 approach tube was centered in the aperture to guide the

Cryomagnetics, Inc. Hall probes mounted in 5/16" O.D. stainless steel rods, as was done in testing the SS1 Type-1 prototype solenoid HINS_SS1_SOL_01 [2].

All current ramps were made at 1 A/s (or less) for this test. Quench training of the solenoid on 11/12 was followed by attempts to measure the solenoid axial magnetic field profile. However, problems with both the axial and transverse Hall probes forced a change of plans, to the study of vertical dipole (VD) quench performance on 11/13, and horizontal dipole (HD) on 11/14. *[DAQ Footnotes: The VD current readout was not initially included in the quench or slow scan readouts. A quench characterization signal "Raw current PS2" was added after the first quench, to capture the PS2 current monitor output (33 A/V). The same current monitor signal was added to the unix slow scan (with the correct shunt calibration added soon after) following the second VD ramp to quench. During the VD and HD testing, the quench currents were visually determined from watching the power supply monitor GUI and written into the stand 3 log book].*

The axial Hall probe was eventually made to work, by adding strain relief on the cable, and the solenoid axial field profile was measured at 100 A. This was followed by a measurement of the axial field at the solenoid center as a function of current, and again in the fringe regions 150 mm above and below the center, to study the effects of iron yoke saturation. The transverse probe could not be made to work, so the correction dipole fields were not captured at operating current. Instead, after the solenoid was warmed up to room temperature, profiles of each dipole were measured with a low excitation current of 0.1 A using a Group3 0.3 T range Hall probe mounted in a 5/16" O.D. carbon fiber tube (which allowed it to be mounted in the same drive system and G10 guide tube). Background fields were significant compared to the solenoid field at this low current, so profiles were also taken with no current in the magnet.

IV. Quench Performance

The quench history of the solenoid is shown in Fig. 12. The magnet trained quickly to the predicted current with plateau quenches in the Main Coil, and early training quenches occurred in both bucking coils. However, after training there were two quench events in the Lead End Bucking Coil (BCL) – the first one while ramping up to 190 A for magnetic measurements, the second while on flat top at 190 A (actual 188.5 A) during quench testing of the Horizontal Dipole. These were unexpected spontaneous quenches after training (and after numerous other ramps to the 190 A level), which makes them somewhat worrisome.

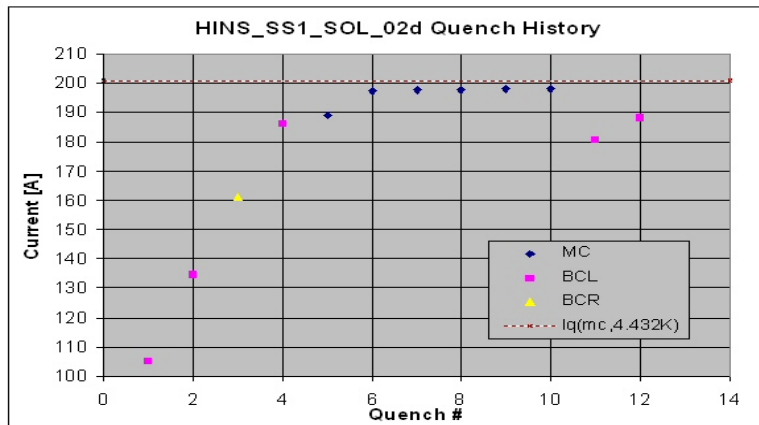


Fig. 12. Quench history of SS1 prototype Type-2 solenoid.

Training of the steering correction dipoles, shown in Fig. 13, was relatively short with only three quenches each. The main solenoid was first ramped to the 190 A level - actually 188.5 A, based upon the Danfysk transducer readout on the Quench Detection (QD) GUI - then one or the other corrector was ramped to quench in the solenoid field. Only the first VD training quench was below the predicted 40 A quench current; both dipoles trained to a slightly higher plateau of about 43 A (Fig. 13 shows the values reported by the PS monitor; the “Raw current PS2” signal recorded by the Quench Characterization (QC) system is typically about 1 A higher – even though it is derived from the same power supply monitor output. Thus, the correction dipole current readout is uncertain at the level of about ± 1 A).

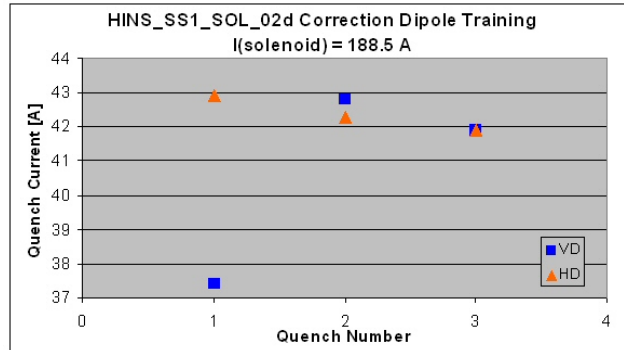


Fig. 13. Quench history of steering correction dipoles.

IV. Solenoid Magnetic Performance

Fig. 14 shows the axial magnetic field transfer function profile compared to the as-built Opera 2D model prediction at 100 A (the field is normalized by the current displayed on the QD GUI, I_{qd} , which was actually 99.2 A). Fig. 15 shows two views of the transition and fringe field regions, illustrating close agreement between data and model, except where the model slightly underestimates the actual field undershoot at the end of the magnet where bucking causes the field to fall rapidly. BCL and BCR have slightly different radial positions: inner radius is 22.5 mm at LE ($Z > 0$) and 22.0 mm at RE ($Z < 0$). This results in a slight field profile difference at about 80 mm from the solenoid center. Qualitatively this agrees with the model prediction; however, the data show much larger field variation than the model in this region: the same phenomenon was previously seen (see Fig. 9 in [2]) and the detailed profile could be matched by adjusting the modeled BC axial positions at the level of a few hundred microns.

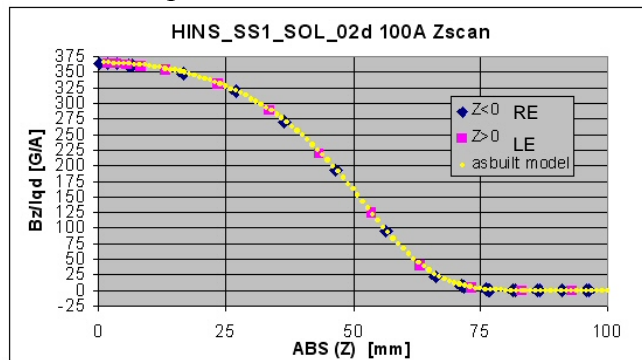


Fig. 14: Comparison of predicted and measured axial magnetic field transfer function at 100A (reflected about the peak position).

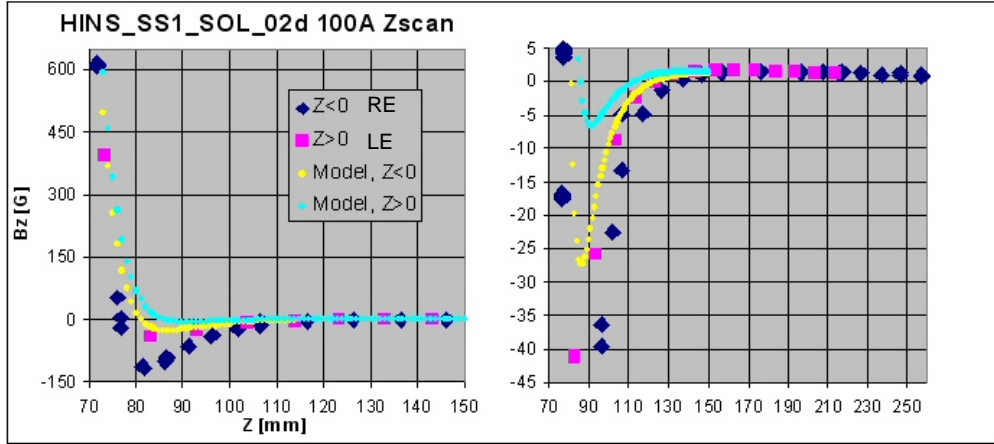


Fig. 15: Detail in fringe regions of predicted and measured axial magnetic field at 100A (the two figures show the same data plotted on different vertical and horizontal scales).

We can conclude here that there is essentially no difference in fringe field outside the solenoid if the BC inner radius is made 22.0 or 22.5 mm.

The current dependence of the central field is shown in Fig. 16. The transfer function is shown there for two different values of the magnet current: I_{qd} is taken from the quench detection GUI display, which is derived from the Danfysk transducer whose accuracy was measured to be within 0.1% of the true current. Because it is only reported to one decimal place, and fluctuates due to noise, the precision of I_{qd} is not as good as the slow scan current readout, I_{unix} , which is derived from the power supply monitor output and is accurate to only 1%. Thus, I_{unix} gives a more precise representation of the trend with current, while I_{qd} is more accurate. The trend at low current is probably due to iron hysteresis effects; the high current variation is quite small and agreement with the model is better than 1%.

At 100A, the measured squared field integral is $\int B^2 dz = 98.5 \text{ T}^2\text{-cm}$, and the required field integral of $300 \text{ T}^2\text{-cm}$ is met at an operating current of $I_{op}=175 \text{ A}$. This implies the current margin $(I_q - I_{op})/I_{op}$ is less than designed: from Fig.3, we expected a quench current of 209 A and current margin of 19 %. At 4.43 K, the quench current of 199 A leads to a margin of 14 %, and at 4.58 K (the minimum helium temperature expected at the HINS beam line in MESON lab), the calculated margin (see Fig. 9) will be only 9 %.

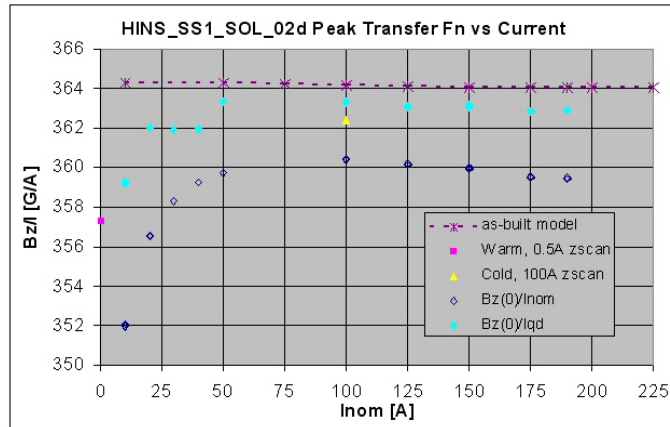


Fig. 16. Transfer function versus current with model prediction at the solenoid center.

The current dependence of the fringe field is shown in Fig. 17, along with a comparison of the model prediction, at 150 mm from the solenoid center. The data are in nice agreement with the prediction, and show that the fields there stay below 2 Gauss up to 175 A (the nominal operating current), above which saturation effects start to become significant and reach the 10 G level at the quench current.

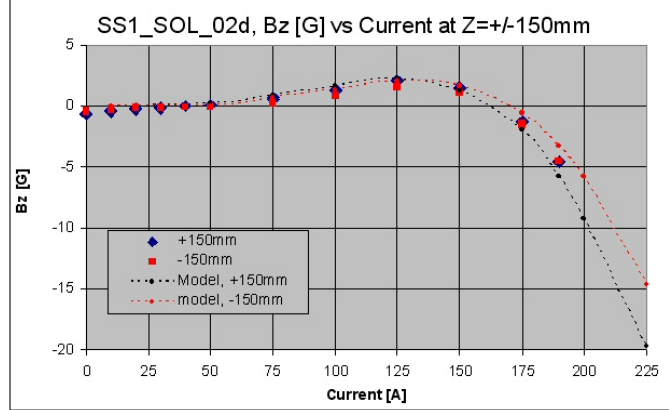


Fig. 17. Measured current dependence of axial magnetic field in the fringe regions, and comparison with model prediction.

V. Steering Dipole Magnetic Performance

The correction dipole package for this prototype SS1 Type-2 solenoid was the first such assembly fabricated, so its magnetic properties are of some interest: we wish to determine the integral field strength, characterize the field uniformity, and measure how well the dipole field angles meet expectations after the magnet was assembled.

On 8/1/08, after initial fabrication of the dipole package, we attempted to estimate the integral field strength and uniformity by making room temperature rotating harmonic coil probe measurements at low current (this was the only option available). Fig. 18 shows the setup: a 25 cm long tangential coil probe of radius 1.22 cm was centered in the dipole package and connected to the (VMTF) vertical drive system which was used to rotate the probe at about 1 Hz. Since the dipoles are about 12 cm long, this probe captures the integrated field at a radius close to the maximum possible (1.5 cm) and thereby characterizes the field quality at all radii less than the probe radius. The probe angles and voltages were recorded using the DSP-based EMS harmonics measurement cart, with gains set to 1000 (which were later calibrated and applied in the analysis). Measurements of over 100 probe rotations were each taken at currents of $\pm 0.10\text{A}$ and $\pm 0.25\text{A}$, in order to remove contributions from background fields (e.g., from the Earth).

Steering Dipole Strengths

The integrated dipole strengths versus current are shown in Fig. 19 for both dipoles. The slopes are similar, and yield transfer functions of 486 and 502 G-cm/A for the VD and HD, respectively. The expected integral strength from [1] is 172 G-cm/A, (for 57 turns per coil, rather than the actual 55), a factor of 2.8 smaller. This large difference in strength is still under investigation. However, in the analysis of harmonics to determine field uniformity, the harmonic coefficients are determined relative to the main field strength (using the same tangential coil on the probe); therefore the uniformity results are not affected by this anomaly.

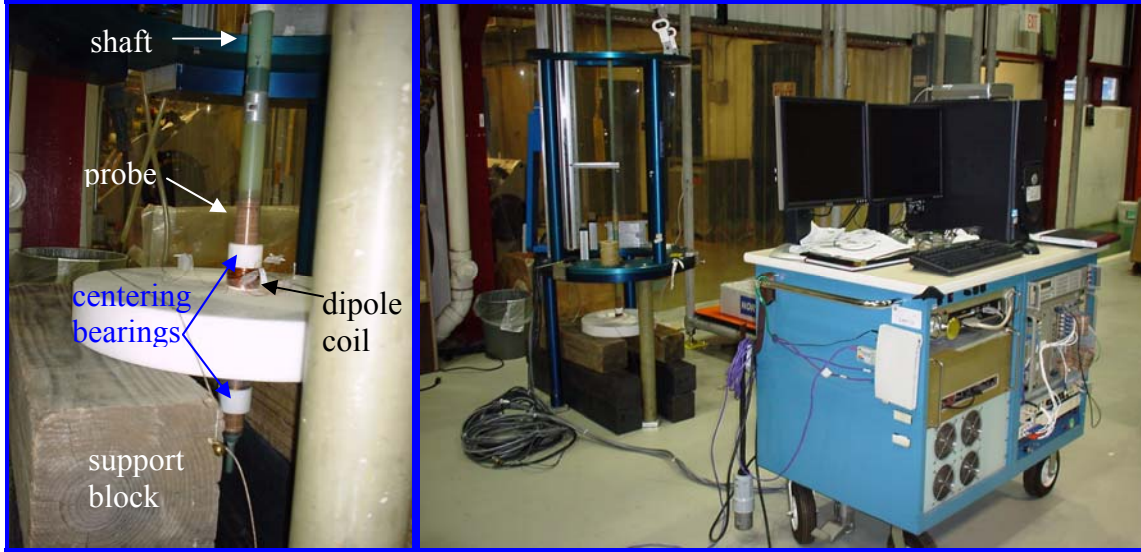


Fig. 18. Harmonic coil probe centered inside supported dipole package (left), vertical drive system and DSP measurement cart (right).

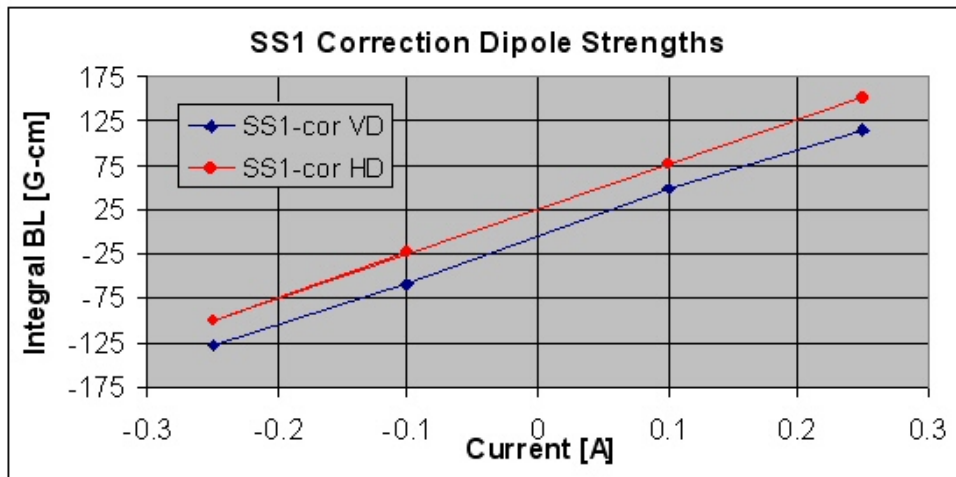


Fig. 19. Warm integrated strength versus dipole current from harmonic coil system.

In addition to the warm harmonic coil measurements, as discussed earlier warm Hall probe measurements were made to capture the field profiles at 0.1 A after the cold test of the assembled magnet. Scans at 0 A were also made to determine the background field levels for subtraction at this low level. Fig. 20 shows the raw data for the VD, and Fig. 21 shows the HD, with the powered and un-powered measurements overlaid. Fig. 22 shows that after subtracting the background level at each z-position, the VD and HD profiles look very similar and symmetric. These Hall probe data yield transfer functions of 212 and 214 G-cm/A for VD and HD, respectively, which are 23% higher than the predicted design value of 172 G-cm/A. Consistent with this, the peak transfer function of 23 G/A (from Fig. 21), is about 21% higher than the predicted 19 G/A (from Fig. 27 in [1]).

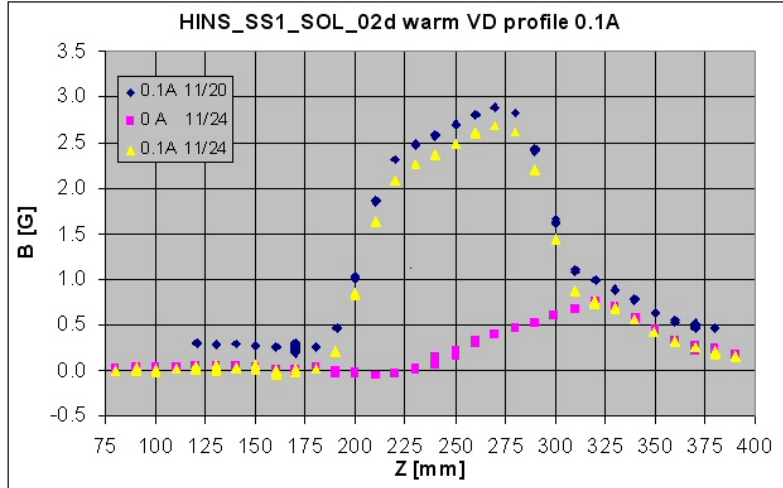


Fig. 20. Vertical Dipole profiles at 0 A and 0.1 A (measured twice)

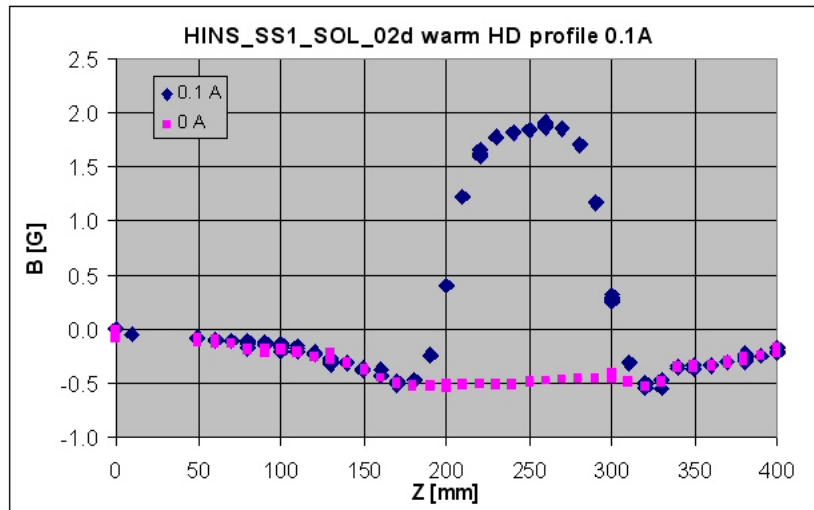


Fig. 21. Horizontal Dipole profiles at 0 A and 0.1 A

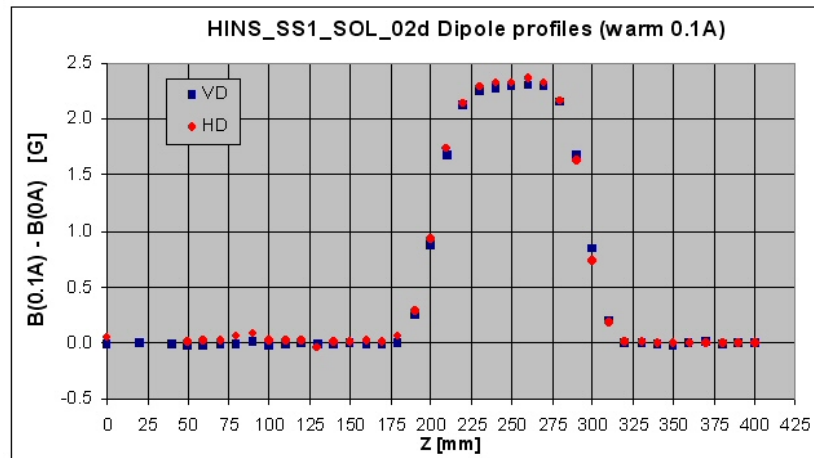


Fig. 22. Vertical and Horizontal Dipole warm transverse field profiles (background field subtracted)

Correction Dipole Field Quality

The 2D model prediction for the magnetic field distribution of the “as-built” steering coils geometry at 40A is shown in Fig. 23 for the Horizontal Dipole, and in Fig. 24 for the Vertical Dipole.

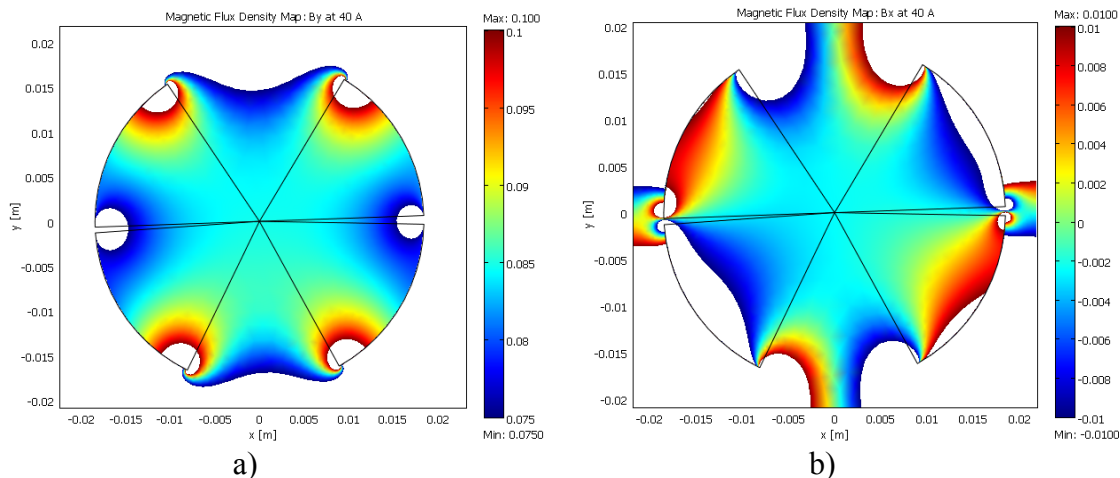


Fig. 23. As-built HD magnetic field (in Tesla) at 40A: (a) B_y and (b) B_x

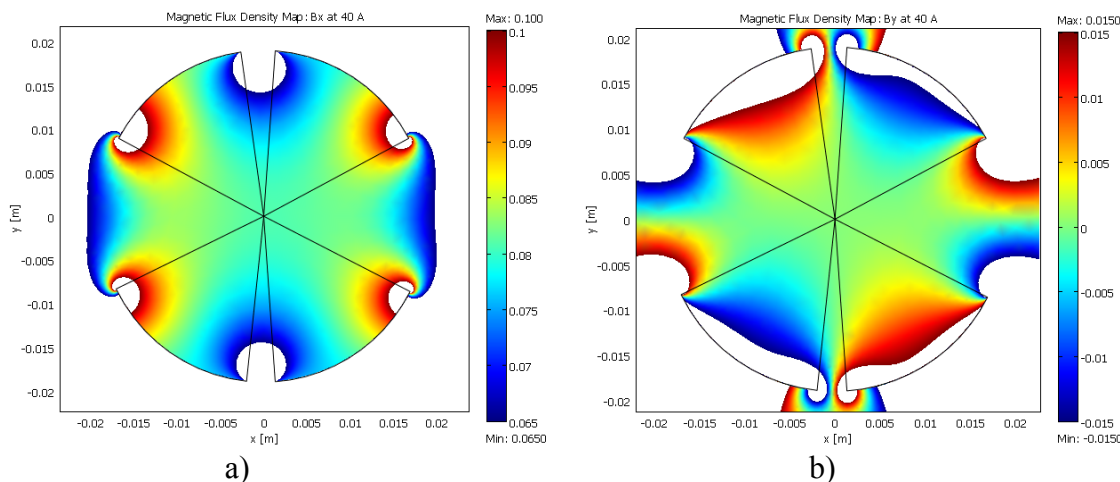


Fig. 24. As-built VD magnetic field (in Tesla) at 40A: (a) B_x , and (b) B_y

As was mentioned earlier, measurements of the magnetic field uniformity were made using a harmonic coil probe. The harmonic coil probe measurements yield field uniformity information, independent of the field strength to which all of the harmonics are normalized. The field components at a given position (x, y) are given by the following harmonic expansion [7]:

$$B_y + iB_x = \sum_{n=1}^{\infty} [B_n + iA_n] \cdot \left(\frac{x + iy}{R_{ref}} \right)^{n-1} \quad (1)$$

where the field coefficients B_n and A_n are reported at the reference radius R_{ref} , which in this case (and by convention in MTF) is 1 inch or 2.54 cm. The normal (b_n) and skew (a_n) harmonic coefficients are equal to the field coefficients normalized by the main

(normal) field strength, and are reported in “units”, where one unit is 10^{-4} of the main field strength (in this case B_1 , which is the normal dipole); thus,

$$\begin{aligned} b_n &= 10^4 \cdot B_n / B_1, \\ a_n &= 10^4 \cdot A_n / B_1. \end{aligned} \quad (2)$$

We can calculate the fractional deviation from the pure dipole field in both the dipole direction, dB_y/B_y , as well as the orthogonal “skew dipole” direction, (dB_x/B_y) . Since harmonics are evaluated up to 15th order, we have::

$$\begin{aligned} dB_y / B_y &= \sum_{n=2}^{15} b_n ((x + iy) / 2.54)^{n-1}, \\ dB_x / B_y &= \sum_{n=2}^{15} a_n ((x + iy) / 2.54)^{n-1}. \end{aligned} \quad (3)$$

Thus, applying Eqn. 3 using harmonics coefficients from the +0.25A coil excitation current, we obtain results shown in Fig. 25 for the HD and Fig. 26 for the VD. In these figures, the “Y” axis (up) is the direction of the main dipole field (B_1 , in Eqn. 1). The measured coefficients are valid for all $(x^2 + y^2) < R_{\text{probe}}^2 = 1.22 \text{ cm}$, so the calculations are made and illustrated with this constraint (that is, we do not extrapolate the field expansion to larger radius, although the solenoid aperture extends to 1.5 cm).

These figures show fractional deviations of more than 10 % in some regions, as well as some tilt in the VD field errors. Further study of the full data set and detailed comparison with predictions is still in progress; additional measurements are planned, including measurements of a second correction dipole package.

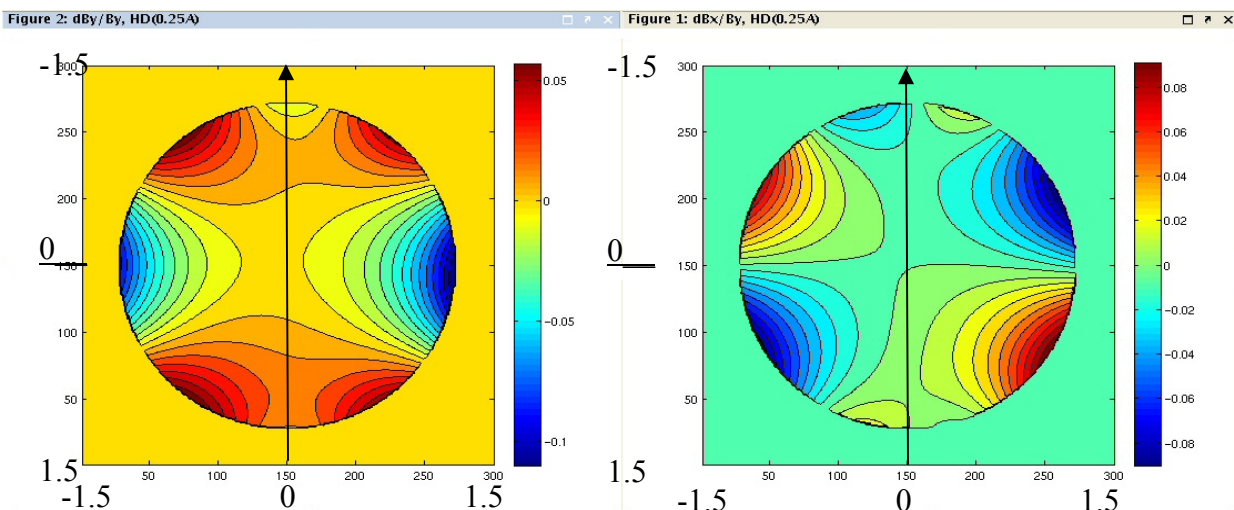


Fig. 25. Field uniformity maps, within probe 1.22 cm radius, for the HD correction dipole reconstructed from warm harmonics measurements at 0.25 A, showing dB_y/B_y (left) and dB_x/B_y (right). Note: Y is up and coordinate ticks are given in units of 0.1mm, with the solenoid center at (150,150) – thus, the figures span $\pm 1.5\text{cm}$ in X and Y.

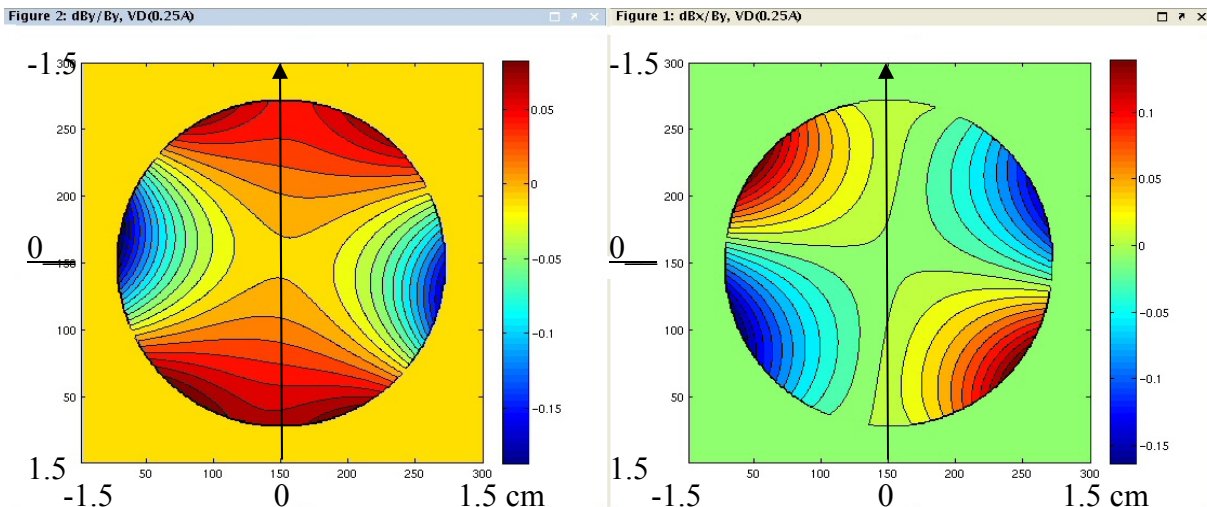


Fig. 26. Field uniformity maps, within probe 1.22 cm radius, for VD correction dipole reconstructed from warm harmonics measurements at 0.25 A, showing dBy/By (left) and dBx/By (right). Note: Y is up and coordinate ticks are given in units of 0.1mm, with the solenoid center at (150,150) – thus, the figures span ± 1.5 cm in X and Y.

Correction Dipole Field Angles

The dipole field angles were measured warm after the cold test, using a device that combines a magnetometer and angle encoder. The absolute vertical field angle is calibrated and precise to about 1 degree. The vertical reference direction is defined by the base of the helium vessel (which will mount on the cryostat support post); the HD angle was found to be +0.45 degrees; the angle between dipoles is 91.2 degrees, which is 1.2 degrees from perfectly orthogonal. However, because this measurement is influenced by the Earth's magnetic field and iron magnetization, the true field angles must be measured at high current, for example using the stretched wire system.

VI. Conclusions

A prototype SS1 Type-2 solenoid was built, and the fabrication followed the specified design closely. Quench performance of the main solenoid and correction dipoles were tested at 4.43 K. In six training quenches, the solenoid reached a plateau of 198 A, just below the expected 201 A. The horizontal and vertical correction dipoles were quench tested in the solenoid field at 190 A. Both coils trained quickly (only one training quench in VD at 37 A) to a current of 42 A, which is slightly above the predicted value of 40 A.

A measurement of the axial magnetic field profile was made at 100 A, and current-dependence of the central and fringe fields were studied. At 100 A the measured central field transfer function is 363 G/A, which is within 1% of the prediction. There is very little dependence of the central field strength on current; the measured transfer function below 25 A dropped about 3 %, which is probably an effect of iron hysteresis. The required field integral of 300 T²-cm is achieved at an operating current of 175 A.

There is very good agreement with the predicted shape and magnitude from the as-built model well beyond the magnet ends where the asymptotic field strength is below 2 G at 100 A. The actual field in the region just beyond the bucking coils disagrees with the model; this feature has previously been observed and can be explained by slight shifts in the BC positions with respect to the nominal as-built positions. At 150 mm from the

center, the axial field remains below 2 G at currents up to 175 A; it grows to about 10 G at 200 A current.

The correction dipole fields were only measured warm, due to probe readout problems during the cold test. Since this dipole is a new design intended to optimize field quality, a harmonic coil system was used to study the strength and harmonics. The field quality looks reasonable at first glance. Further work is needed to understand the strength discrepancy seen with the harmonic coil system, and to fully examine the field uniformity. The dipole field profiles were also measured warm by scanning with a sensitive Hall probe with and without current in the dipoles, and making a background subtraction. The resulting profiles look very similar and symmetric, with measured peak transfer functions of about 23 G/A and field integrals of 213 G-cm/A – compared to the design values of 19 G/A peak and 172 G-cm/A integral. Thus, the correction dipoles should achieve the required 0.5 T-cm field integral at an operating current of 23.5 A, which allows plenty of operating current margin (quench at ~40 A). The horizontal and vertical dipole field angles were measured warm with respect to alignment scribe marks, using a new angle encoding magnetometer system. They were found to be oriented with respect to the alignment axis, and orthogonal to each other, within about 1 degree.

This solenoid is a viable lens for use in the HINS beam line, although the operating margin is somewhat less than expected: it is 19 % at 4.2 K, but only 9 % when taking into account the expected helium temperature (4.6 K) at the Meson lab. Having the desire to increase the operating margin, some slight design changes will be made and tested with a pre-production model. In the near future, the plan for this prototype solenoid is to assemble it into a liquid helium vessel and mount it in the SSR1 Test Cryostat to study the effectiveness of magnetic shielding, which is designed to reduce the few-Gauss fringe fields to less than 10 μ T at adjacent SCRF cavity walls. Beyond this, its use in studies of solenoid alignment in SS1 cryostats are anticipated.

References

- [1] G. Davis, M. Tartaglia, I. Terechkine, J. Tompkins, T. Wokas, “HINS Linac SS-1 Section Prototype Focusing Solenoid Design,” TD-08-010, FNAL, March 31, 2008.
- [2] G. Davis, C. Hess, S. Kotelnikov, F. Lewis, A. Makulski, D. Orris, R. Rabehl, M. Tartaglia, I. Terechkine, J. Tompkins, T. Wokas, “HINS_SS1_SOL_01 Fabrication Summary and Test Results,” TD-08-012, FNAL, April 22, 2008.
- [3] L. Bottura, “A practical fit for the critical surface of NbTi,” *IEEE Trans. Appl. Supercond.*, Vol. 10, No. 1, pp. 1054-1057, 2000.
- [4] V. Veretennikov, I. Terechkine, “HINS Front End SS-1 Section Focusing Solenoid Quench Protection Analysis”, FNAL TD-07-020, FNAL, TD, Aug. 2007
- [5] I. Terechkine, V. Veretennikov, “Normal Zone Propagation in Superconducting Focusing Solenoids and Related Quench Protection Issues”, *IEEE Transaction on Applied Superconductivity*, v. 18, NO. 2, pp. 1325 – 1328, June 2008.
- [6] I. Terechkine, “Quench Protection Study for Focusing Solenoids of Superconducting Sections of HINS Linac,” TD-09-002, FNAL, February 2009.
- [7] A. Jain, “Harmonic Coils,” CERN Accelerator School on Measurement and Alignment of Accelerator and Detector Magnets, Anacapri, Italy, 1997; CERN Report 98-05, pp. 175-217.